



**HAL**  
open science

# Hygroscopic stresses in asymmetric biocomposite laminates submitted to various relative humidity conditions

Mael Péron, Amandine Céline, Frédéric Jacquemin, Antoine Le Duigou

► **To cite this version:**

Mael Péron, Amandine Céline, Frédéric Jacquemin, Antoine Le Duigou. Hygroscopic stresses in asymmetric biocomposite laminates submitted to various relative humidity conditions. *Composites Part A: Applied Science and Manufacturing*, 2020, 134, pp.105896 -. 10.1016/j.compositesa.2020.105896 . hal-03490918

**HAL Id: hal-03490918**

**<https://hal.science/hal-03490918>**

Submitted on 20 May 2022

**HAL** is a multi-disciplinary open access archive for the deposit and dissemination of scientific research documents, whether they are published or not. The documents may come from teaching and research institutions in France or abroad, or from public or private research centers.

L'archive ouverte pluridisciplinaire **HAL**, est destinée au dépôt et à la diffusion de documents scientifiques de niveau recherche, publiés ou non, émanant des établissements d'enseignement et de recherche français ou étrangers, des laboratoires publics ou privés.



Distributed under a Creative Commons Attribution - NonCommercial 4.0 International License

# Hygroscopic stresses in asymmetric biocomposite laminates submitted to various relative humidity conditions

Mael Péron<sup>1,\*</sup>, Amandine Céline<sup>1</sup>, Frédéric Jacquemin<sup>1</sup>, Antoine Le Duigou<sup>2</sup>

1: Université de Nantes

GeM, Institut de Recherche en Génie Civil et Mécanique, Equipe E3M

58 rue Michel Ange, BP420, 44600 Saint-Nazaire - France

2: Univ Bretagne-Sud

IRDL UMR CNRS 6027, Pole Thématique Composite,

Rue Saint-Maudé, B 92 116, 56321 Lorient Cedex - France

\*Corresponding author: [mael.peron@univ-nantes.fr](mailto:mael.peron@univ-nantes.fr)

## Abstract

Hygroscopicity of natural fibers influences biocomposites lifetime submitted to wet environments. The present study investigates the hygroscopic stresses state in a flax fiber reinforced polypropylene composite when submitted to different environmental conditions from the dried state through various relative humidity (RH) to immersion. An experimental and modelling strategy is applied on asymmetric biocomposites to estimate the stresses distribution through their thickness.

On dry condition, transverse tensile stresses reached 26.4MPa. These stresses were nullified at 50%RH and then increased again until 90%RH or immersion conditions are applied. The evolution of the internal stresses influence drastically the tensile strength of biocomposites. Indeed, the internal stresses overcome the transverse strength of Flax/MAPP unidirectional ply, which potentially leads to damage. Environmental loading and gradient effect also drastically influence the internal stresses. A progressive humidification step enables to reduce drastically the stresses intensity with levels lower than 10 MPa thanks to lower hygroscopic gradients.

**Keywords:** A. Natural fibers; B. Internal stresses; C. Laminate mechanics; D. Moisture

## 1. Introduction

The use of natural fibers as a reinforcement for composite materials has known a growing use over the past decades due to their interesting mechanical performances and low environmental impact compared to glass fibers. However, these fibers possess hydrophilic components, leading to important moisture absorption (reaching 25% under 95% RH [1]) and anisotropic hygroscopic expansion. This hygroscopic behavior has to be considered when designing composite parts, as it may contribute to part deformation and internal stresses development. The transverse hygroscopic expansion of a single flax fiber is linked to its microstructure, which is driven by its microfibril angle and its biochemical composition. This expansion attains 21% under 95% RH condition when the fiber is free of swelling [2], but reaches “only” 3.2% for a composite made of 60% in volume of flax fibers and PP matrix when submitted to immersion conditions [3].

Despite an important fiber volume fraction, this decrease in hygroscopic swelling is caused by the contrast of hygro-mechanical behavior between the fibers and the surrounding polymer matrix. This latter is often less sensitive to moisture sorption and induces a constraining effect on the fibers by reducing their hygroscopic swelling. This leads to a compressive state in the radial direction of the fibers, which reduces the fiber free expansion and potentially increases the load transfer between the fibers and the matrix [2,4]. This compressive stress state also leads to a lower access of the fibers to the moisture diffusion [3,5,6]. Despite these positive aspects, the contrast of hygroscopic swelling behavior between natural fibers and the surrounding matrix was shown to be a major source of damage within the composite, which reduces the material lifetime [7]. This behavior difference is often cited to initiate matrix cracking, fiber/matrix interface debonding or even ply delamination [7–9].

The estimation of induced stresses states in composite materials can be performed through experimental or numerical approaches. Numerous experimental approaches have been developed in the past decades to estimate induced stresses in composite materials [10]. Among them, the study of asymmetrical laminates submitted to environmental variations leads to simple identification of the material residual strains through the measurement of its out-of-plan deflection, but it relies on the use

of a model to estimate the stresses distribution in the laminate [3,11,12]. Numerical approaches were developed to investigate the development of hygro-mechanical stresses in synthetic fibers reinforced composites [5,13–19] and only few approaches are found on biocomposites [3,20,21]. Also, these numerical approaches have to be validated by comparing their results with experimental measurements. Therefore, a complete method including both an experimental and a modelling approach is necessary to validate the developed model and estimate the stresses distribution in the composite. This was proposed by the authors in a previous study [3], which was however limited to the investigation of immersion conditions from a sample initially submitted to 50%RH. Immersion is a severe environment, which might not be representative of the real use conditions of biocomposites. Also, this study did not focus on the dried state of the material, neither on its mechanical behavior under low RH conditions. A more recent study proposed to identify the hygro-mechanical behavior of the same material, but it only proposed an estimation of the composite deformation under several relative humidity conditions. Finally, the model developed in [3] was validated by comparing the predicted curvature of an asymmetric laminate in its fully saturated state with the experimentally measured one, but the evolution of the curvature during sorption was not discussed. The validation of the model during transient moisture diffusion is still to be performed. It therefore appears that the study of the impact of various relative humidity on the hygroscopic stresses of a flax fiber reinforced composite material has never been proposed in the literature and deserves a complete investigation.

The present study proposes to investigate the development of hygroscopic stresses in a flax fiber reinforced polypropylene matrix composite when submitted to different environmental conditions, from the dried state (RH 0%) to immersion through various relative humidities (10, 30, 50, 70 and 90%). It aims at estimating the induced hygro-mechanical strains and stresses state in an asymmetric bilaminar composite strip, which has been previously characterized [22]. The data collected in this previous study is used to feed a hygro-mechanical model [3] which is adapted to the study of asymmetrical thin plates submitted to relative humidity conditions. The model permits to estimate the deformations of the asymmetric laminate, which are compared with the experimentally measured ones. Then, the stress distributions through the thickness of the laminate are estimated under several

environmental conditions. Finally, the estimated stress distributions and values are discussed regarding experimental investigations performed on the material.

## 2. Materials and Methods

### 2.1. Materials

Flax fibers (*Linum usitatissimum*) were harvested in France, before being dew retted, scutched and hackled. Unidirectional (UD) flax fibers tapes (of areal densities 200 g/m<sup>2</sup> and 50g/m<sup>2</sup>) were supplied by *Lineo*. Extruded and film-cast Maleic Anhydride compatibilized PolyPropylene (MAPP PPC 3660 from Total Petrochemicals) were used to manufacture the MAPP/flax laminates. Stacks of polymer films and unidirectional flax fibers tapes were prepared in a metallic mold (of in-plane dimensions 130 x 130 mm<sup>2</sup>). The laminate were manufactured with a dedicated hot pressing protocol, consisting in a dwell step at 190°C for 8 min under 20 bars, with an incrementally applied pressure to maintain the alignment of the fibers. It was then cooled to room temperature at a 15°C/min rate. The targeted fiber volume fraction was set to 60% in volume. The resulting porosity was 1.35% ± 0.2% in volume [22].

Several stacking sequences were used in [22] to characterize the hygro-mechanical behavior of the material, including [0°]<sub>14</sub>, [90°]<sub>26</sub> and [+45/-45]<sub>8s</sub>. These lay-up sequences were selected in order to characterize the longitudinal modulus  $E_L$ , the transversal modulus  $E_T$  and the in-plane shear modulus  $G_{LT}$ , respectively. These properties were estimated through tensile tests and range from the highest value to the lowest [22]. The thickness of the samples used to identify them had to evolve inversely so the stiffness of all the samples would be of the same order of magnitude. An asymmetric stacking sequence laminate was also manufactured, following a [0<sub>1</sub> 90<sub>5</sub>] stacking sequence which permits to emphasize the out-of-plane bending of the laminate [23,24]. The obtained dimensions for this last laminate were 70 x 10 x 0.46 mm<sup>3</sup>. More details concerning the preparation of the specimens can be found in [22].

## 2.2. Modelling

The hygro-mechanical model previously developed by the authors [3] permitted to well describe the hygro-mechanical behavior of the composite when submitted to immersion condition. In the present study, it is adapted and applied to the investigation of the material behavior submitted to various relative humidity conditions. This model is based on a unidirectional description of the moisture diffusion through the thickness of the laminate solved by a finite difference scheme, and on the modified lamination theory to translate the mechanical behavior of the composite. Both models are weakly coupled, as the water diffusion impacts the hygroscopic swelling and mechanical properties of the composite but the stress state does not affect the moisture diffusion.

According to the previously observed moisture diffusion kinetics in similar materials [3,25], it appears they can be approached by a Fickian law (Eq. 1).

$$\frac{\partial C(z, t)}{\partial t} = \nabla_z D_{zz} \nabla_z C(z, t) \quad (\text{Eq. 1})$$

$$C(-h, t) = C(h, t) = C_{imp} \quad (\text{Eq. 2})$$

$$C(z, 0) = C_0 \quad (\text{Eq. 3})$$

where  $C$  is the moisture content field,  $t$  is the time,  $z$  is the through thickness coordinate,  $\nabla_z$  is the spatial differential operator along the  $z$  direction,  $D_{zz}$  is the moisture diffusion coefficient in the through-thickness direction,  $h$  is the half thickness of the laminate,  $C_0$  and  $C_{imp}$  are the initial and imposed moisture contents, respectively. The prescribed content and the initial conditions are given by Eqs. 2 and 3 respectively. This problem is solved by the finite difference method in *Matlab R2017a*. It leads to the evolution of the mean moisture content value and its distribution through the thickness of the laminate.

The hygro-mechanical behavior of the material is expressed through a linear hygro-elastic constitutive law. Due to the low thickness of the studied laminates, it is expressed following a plane-stress assumption:

$$\begin{Bmatrix} \sigma_{xx} \\ \sigma_{yy} \\ \sigma_{xy} \end{Bmatrix} = \begin{bmatrix} Q_{11} & Q_{12} & Q_{16} \\ Q_{12} & Q_{22} & Q_{26} \\ Q_{16} & Q_{26} & Q_{66} \end{bmatrix} \left( \begin{Bmatrix} \varepsilon_{xx} \\ \varepsilon_{yy} \\ \varepsilon_{xy} \end{Bmatrix} - \begin{Bmatrix} \varepsilon_{xx}^{hyg} \\ \varepsilon_{yy}^{hyg} \\ \varepsilon_{xy}^{hyg} \end{Bmatrix} \right) \quad (\text{Eq. 4})$$

where  $\sigma_{ij}$  are the components of the stress tensor expressed according to the plane-stress assumptions,  $Q_{ij}$  are the components of the reduced stiffness tensor of the material in the global coordinate system  $(x, y, z)$  of the laminate [26] which are deduced from the identified material properties  $E_L$ ,  $E_T$ ,  $\nu_{LT}$  and  $G_{LT}$ .  $\varepsilon_{ij}$  and  $\varepsilon_{ij}^{hyg}$  are the in-plane components of the total and hygroscopic strain tensors respectively. It has to be noted that the components of the reduced stiffness tensor and of the hygroscopic strain tensor depend on the current moisture content  $C_{mean}$  which corresponds to the mean value over the ply thickness, deduced from the moisture distribution  $C$  obtained with the finite difference scheme.

Considering the relatively low thickness of the studied plates compared to their in-plane dimensions as well as the asymmetric ply sequence, the modified lamination theory proposed by Hyer [27] was felt as well suited to model the hygroscopic behavior of the studied laminates. This method is based on a postulate of the displacement field  $(u, v, w)$  along the three directions of the global coordinate system  $(x, y, z)$ . The form of the field is chosen to reproduce the experimentally observed shapes of deformed asymmetric laminates. Its out-of-plane component  $w$  is expressed as:

$$w = \frac{1}{2}(ax^2 + by^2) \quad (\text{Eq. 5})$$

where  $x$  and  $y$  are the in-plane general coordinates of the laminate,  $a$  and  $b$  are the curvatures of the laminate along the  $x$  and  $y$  direction, respectively. From the displacement field and according to the Kirchhoff hypotheses, the in-plane strain components are determined with non-linear strain-displacement relationships, following the von Karman approximation of Green's strain measure:

$$\varepsilon_{xx} = \frac{\partial u}{\partial x} + \frac{1}{2} \left( \frac{\partial w}{\partial x} \right)^2 - z \frac{\partial^2 w}{\partial x^2} \quad (\text{Eq. 6})$$

$$\varepsilon_{yy} = \frac{\partial v}{\partial y} + \frac{1}{2} \left( \frac{\partial w}{\partial y} \right)^2 - z \frac{\partial^2 w}{\partial y^2} \quad (\text{Eq. 7})$$

$$\varepsilon_{xy} = \frac{1}{2} \left[ \frac{\partial u^\circ}{\partial y} + \frac{\partial v^\circ}{\partial x} + \left( \frac{\partial w}{\partial x} \right) \left( \frac{\partial w}{\partial y} \right) \right] - z \frac{\partial^2 w}{\partial x \partial y} \quad (\text{Eq. 8})$$

where  $u^\circ$  and  $v^\circ$  are the mid plane displacements along the  $x$  and  $y$  directions, respectively. The components of the strain tensor directly feed the constitutive law given in (Eq. 4). Then, the total potential energy  $W$  of the laminate can be expressed following Eq. 9.

$$W = \frac{1}{2} \int_V \sigma_{ij} \varepsilon_{ij} dV \quad (\text{Eq. 9})$$

where  $V$  is the total volume of the laminate. The mechanical equilibrium of the laminate is obtained by minimizing its potential energy  $W$ . This is performed by finding values of the kinematic parameters (*i.e.* the curvatures  $a$  and  $b$ , as well as other parameters used to describe the fields  $u^\circ$  and  $v^\circ$ ) so that the first variation of  $W$  is zero. The minimization of  $W$  can lead to several solutions, each corresponding to an equilibrium shape. It is associated with a stability criterion, which consists in the second derivative of  $W$ . If this latter is positive, then the solution is stable, and *vice-versa*. Once the different values of  $a$ ,  $b$  and the other parameters are determined for a given situation, the strain and stress distributions are computed through the thickness of the laminate by using Equations 6-8 and 4. This distribution can be given either in the global coordinate system ( $x, y, z$ ) or in the local coordinate system of each independent ply ( $1, 2, 3$ ). In the case of a unidirectional ply, the  $1$  direction corresponds to the longitudinal direction of the fibers,  $2$  to the transversal in-plane direction, and  $3$  to the through-thickness direction. This latter is therefore the same as  $z$ . The whole resolution procedure is performed in the *Symbolic Math* toolbox in *Matlab R2017a*. More details concerning the developed model or the modified lamination theory can be found in [3] and [27], respectively.

### 2.3. Hygro-mechanical behavior and properties

A good comprehension of the material hygro-mechanical behavior is mandatory to estimate and understand the induced hygroscopic stresses. Also, the identification of the through-thickness coefficient of diffusion  $D_{zz}$ , the moisture content  $M_{RH}$ , the in-plane elastic moduli  $E_L$ ,  $E_T$  and  $G_{LT}$  as

well as the in-plane hygroscopic strains  $\varepsilon_L^{hyg}$  and  $\varepsilon_T^{hyg}$  and their evolution with the moisture content  $C$  are necessary to feed the developed model. The characterization of the involved material has already been performed and discussed in [3,22]. Their identification is quickly reminded here as it will be useful to understand the generated mechanical state but it will not be further discussed. A continuous description of the evolution of the elastic moduli and hygroscopic strains with the moisture content is proposed in this study in order to describe the behavior of the material submitted to various environmental conditions.

### ***Moisture diffusion and sorption***

The moisture sorption under stationary states was assessed by using a Dynamic Vapor Sorption device (DVS, from Hiden Isochema Ltd, UK) [22]. Sorption and desorption isotherms were obtained from the composite under relative humidity conditions from dry state to 90% RH with intervals of 10% RH. The equilibrium weight recorded for a given condition is denoted as  $W_{RH}$  for a given RH condition. The moisture content for a given RH  $M_{RH}$  was then obtained as the relative difference with the dry condition weight  $W_0$ :

$$M_{RH}(\%) = \frac{W_{RH} - W_0}{W_0} \cdot 100 \quad (\text{Eq. 10})$$

Although achieved in different conditions, immersion tests presented in [3] allowed to complete the sorption study performed by Le Duigou *et al.* [22]. The steady state moisture content during immersion was found to be 31.1%, with a diffusion coefficient  $D_{zz} = 9.6 \cdot 10^{-7} \text{ mm}^2/\text{s}$ . This coefficient is considered as constant for the different environmental conditions. The different moisture contents at steady state obtained with the DVS measurements under several environmental conditions and during the immersion test are summed up in Table 1.

### ***Mechanical Characterization***

The mechanical properties ( $E_L$ ,  $E_T$  and  $G_{LT}$ ) of the biocomposite obtained in [22] for several environmental conditions are presented in Fig. 1. The values given for a moisture content  $C = 31.1\%$  correspond to immersion tests. The different moduli highly decrease with  $C$ , due to the high sensitivity

of the flax fiber mechanical behavior on the moisture content [28]. Identical exponentially decreasing properties were already identified for natural and inorganic fiber composites [19,29].

Based on the measured properties, exponential approximations are proposed in this study to best fit the experimental data. The in-plane elastic moduli  $E_L$  and  $E_T$  were fitted thanks to equation 11 and 12, respectively. The parameters feeding these equations are gathered in Table 2.

$$E_L = E_{L \min} + (E_{L \max} - E_{L \min}) \exp(-0,17 \cdot C) \quad (\text{Eq. 11})$$

$$E_T = E_{T \min} + (E_{T \max} - E_{T \min}) \exp(-0,35 \cdot C) \quad (\text{Eq. 12})$$

Concerning the shear modulus  $G_{LT}$ , the values proposed in [22] only reach a moisture content of  $C = 9.4\%$  due to tests achieved only in relative humidity environment. A linear interpolation is proposed by the same authors [22], but it would lead to negative values of  $G_{LT}$  if extrapolated above  $C = 23\%$ . Therefore, an evolution similar to that of  $E_L$  and  $E_T$  is proposed here. The modulus observed at  $C = 31.1\%$  corresponds to approximately 25% of the initial modulus. An identical decrease is proposed for  $G_{LT}$ , and as a consequence the estimated value at  $C = 31.1\%$  reaches 362 MPa. This value is represented in Figure 1c, and named " $G_{LT \text{ extrap.}}$ ". From the measured and extrapolated value of  $G_{LT}$ , an exponential fitting function is then proposed through Eq. 13.

$$G_{LT} = G_{LT \min} + (G_{LT \max} - G_{LT \min}) \exp(-0,1 \cdot C) \quad (\text{Eq. 13})$$

The fitted values obtained from Eqs. 11-13 are also plotted in Fig. 1. Finally, the in-plane Poisson's ratio  $\nu_{LT}$  is considered as constant and equal to 0.33 [3]. More details concerning the analysis and discussion of the mechanical properties of the biocomposite can be found in [22].

### ***Hygroscopic Expansion***

The measured hygroscopic expansion strains  $\epsilon^{hyg}$  obtained in [22] are represented in Fig. 2 versus the mean moisture content obtained at saturation for several hygroscopic conditions. The longitudinal strains are considered as evolving linearly with  $C$  [3], from 0 to the maximal value of -0.17% obtained

at  $C = 31.1\%$ . It was more difficult to find a simple mathematical function describing the evolution of the transversal strain. Therefore, it was interpolated using a piecewise cubic interpolation function in *Matlab R2017a*. The interpolated values for both directions are shown in Fig. 2. The evolution with the mean moisture content is different compared with values obtained under immersion condition in transient state [3], which can be explained by the presence of important moisture content gradients in partially saturated samples, leading to properties and strains gradients.

### ***Bending curvature***

The evolution with time of the measured bending curvature of the  $[0_1 90_5]$  laminate for each environmental condition is represented in Fig 3a. It is decomposed in two phases: a rapid increase of the curvature followed by a plateau at which the maximum curvature is reached. The maximum values of the curvature for each conditions are represented in Fig. 3b versus the moisture content. It appears that, when plotted against the moisture content  $C$  (Fig. 3b), the curvature highly rises until  $C$  reaches 10% and then stabilizes. This is explained by the evolution of the hygroscopic strain obtained in Fig. 2.

The stabilized recorded profiles of the bending laminate obtained in [22] for the different environmental conditions show almost a straight configuration at 50%RH, which will be considered as the reference situation. Therefore, the hygroscopic strains  $\varepsilon_{ij}^{hyg}$  used in the constitutive law (Eq. 4) will be shifted to consider null values when  $RH = 50\%$ . This leads to  $\varepsilon_{ij}^{hyg} = \varepsilon_{ij}^{hyg\ measured} - \varepsilon_{ij}^{hyg}(RH = 50\%)$ .

## **3. Numerical results**

The model developed in [3] and fed with the properties identified in [22] first permits to estimate the curvature of the asymmetric laminate experimentally observed in [22] and [3]. This permits to validate the model and consider the estimated stresses distributions are correct. First, the validation is presented. Then, the estimated stresses distributions are presented and discussed.

### 3.1. Curvatures

The evolution of the predicted curvatures with time is represented in Fig. 3a for the different environmental conditions when the sample is initially dry. The final values are in good agreement for the different conditions as previously seen, but the predicted increase rate during the early moments of the evolution seems slower than the experimentally observed one, except for the low RH (10 and 30%) and the 90% RH conditions. The steady-state curvatures obtained for each condition are represented in Fig. 3b and compared with the experimentally measured ones. An excellent agreement is found for low moisture content (from 0 to 5%), with less than  $4.10^{-3} \text{ mm}^{-1}$  of deviation between the numerical and the experimental results. The model overestimates the curvature of the composite for the 90%RH and the immersion condition, corresponding to moisture content of 9.46% and 31.1%, respectively, with deviations ranging between  $13.10^{-3}$  and  $14.10^{-3} \text{ mm}^{-1}$ .

The evolution of the curvature measured in [3] on a similar asymmetric laminate from an initial state under 50% RH submitted to immersion condition is represented in Fig. 4 together with the curvature predicted thanks to the initial model [3] and to the adapted model developed in the present study. The measured curvature evolves following an initial linear increase from 0 to  $0.07 \text{ mm}^{-1}$  when  $C$  varies from 2.94% to 10%, followed by a saturation plateau when  $C$  further increases. It attains a final value of  $0.0795 \text{ mm}^{-1}$  at saturation. The initially estimated curvature [3] evolves in a bilinear way, with a slope change occurring by  $C = 14.5\%$ . The slope however remains in the same order of magnitude, which is due to the evolution of the hygroscopic strains measured during the immersion of the composite [3]. The estimated final value reaches  $0.088 \text{ mm}^{-1}$ , which was found to be satisfactory compared to the experimentally measured one as it represents 10.7% of error. The estimated curvature from the developed model evolves also following two regimes. At first, it evolves linearly with  $C$  from 0 to  $0.07 \text{ mm}^{-1}$  when  $C$  rises from 2.94% to 15.6%. It then slowly increases to its final value of  $0.0835 \text{ mm}^{-1}$  at saturation. The final curvature is therefore predicted with an error of 5.0%.

### 3.2. Steady state stresses distributions

The stresses distribution through the thickness of the laminate under the different environmental conditions is given in Fig. 5a and b in the global coordinate system ( $x, y, z$ ). The global coordinate system is pictured in Fig. 6, together with the local one. At RH lower than the reference condition (RH < 50%), the  $0^\circ$  ply slightly expands and the  $90^\circ$  plies shrink along the  $x$  direction. This heterogeneous behavior between plies lead to a bending moment which generates the observed negative curvature along the  $x$  axis (Figs. 3 b). The expansion of the  $0^\circ$  ply is blocked by the  $90^\circ$  plies, which leads to compressive stresses in the  $0^\circ$  ply (Fig. 5a). On the opposite, the  $90^\circ$  plies see their shrinkage blocked by the  $0^\circ$  ply, which leads to a mostly tensile stress. The bending of the laminate leads to a mixed compressive-tensile stress distribution through the thickness of the  $90^\circ$  plies.

Inversely, along the  $y$  direction (Fig. 5b), the  $0^\circ$  ply shrinks and the  $90^\circ$  plies slightly swell. The  $0^\circ$  ply is however blocked by the  $90^\circ$  plies, leading to important tensile stresses. The  $90^\circ$  plies are on the contrary mainly submitted to a compressive stress distribution as their shrinkage is blocked by the  $0^\circ$  ply. At higher RH (> 50%), the  $0^\circ$  ply slightly shrinks and the  $90^\circ$  plies expand along the  $x$  direction. Both directions block one another, leading to tensile stresses in the  $0^\circ$  ply and mainly compressive stresses in the  $90^\circ$  ones. Along the  $y$  direction, the  $90^\circ$  plies tend to shrink whereas the  $0^\circ$  ply swells. This generates compressive stresses in the  $0^\circ$  ply and mostly tensile stresses in the  $90^\circ$  ones.

The stresses in the local coordinate system are easily deduced from the stresses distributions in the global coordinate system. For the  $0^\circ$  ply, the directions  $1$  and  $2$  correspond to the  $x$  and  $y$  directions respectively. For the  $90^\circ$  ply, the directions  $1$  and  $2$  correspond to  $y$  and  $x$ , respectively (Fig. 6). These stresses are represented in Fig. 7a and b for the different environmental conditions. For low RH values (< 50%), the plies are mostly submitted to compressive stresses along their longitudinal direction (Fig. 7a) and to tensile stresses along their transversal direction (Fig. 7b). On the opposite, for high RH values, the plies are submitted to tensile stresses along their longitudinal direction (Fig. 7a) and to compressive stresses along their transversal direction (Fig. 7b). These stresses distributions at high moisture content were also explored by the authors in [3] for laminates submitted to immersion condition.

### 3.3. Transient stresses distribution

The stresses distribution during transient moisture diffusion is also predicted thanks to the developed model. As an example, the case of moisture induced stresses from dry state to saturation under a 90% RH is discussed. The evolution of the mean moisture content  $C_{mean}$  with the square root of time is presented in Fig. 8a, with several specific times  $t_i$ , which are given in Table 3. As the diffusion process is described with a Fickian model, it represents two main phases: a first linear evolution of the mean moisture content with the square root of time from 0 to 15 min<sup>1/2</sup>, followed by a saturation plateau. The moisture content distribution through the thickness for each specific time  $t_i$  is represented in Fig. 8b. For the initial time  $t_0$ , the moisture content is null through the whole thickness. For early times ( $t_1$  and  $t_2$ ), moisture starts to diffuse from the outer surface of the laminate when the core of the laminate remains dry. After  $t_2$  the moisture starts to reach the core of the laminate. For later times ( $t_3$ ,  $t_4$  and  $t_5$ ), the moisture content tends to a homogeneous distribution reaching the saturation value of 9.46%.

The evolution of the stresses distributions in the global coordinate system under 90% RH are given in Fig. 9a and b for the different times  $t_i$ .

The stresses distribution at time  $t_0 = 0$  min corresponds to the completely dry state and was already discussed in the previous sub-section. At time  $t_1 = 3.5$  min, the moisture starts diffusing in the external plies (Fig. 8b). Along the  $x$  direction (Fig. 9a), it leads to a compressive stress in the external 90° plies (from  $z = -0.23$  mm to  $z = -0.2$  mm) as they tend to start swelling but are blocked by the other plies situated closer to the laminate center. Along the  $y$  direction (Fig. 9b), it also leads to compressive stresses in the 0° ply (from  $z = 0.22$  to  $z = 0.23$ mm) for the same reason. The important variation of stresses distribution in the 0° ply is accompanied by a decrease in the intensity of the stresses in the 90° plies for both tensile and compressive stresses. At time  $t_2 = 31.5$  min, the moisture diffusion progresses to the center of the laminate (Fig. 8b). The observation from  $t_1$  along the  $x$  direction holds. Along the  $y$  direction (Fig. 9b), most of the 0° ply is now submitted to a compressive stress as it tends to swell but is blocked by the 90° plies. Most of these latter plies are therefore submitted to tensile stresses to reach the mechanical equilibrium of the laminate. At time  $t_3$ , the stresses along the  $x$  direction exhibit a nearly symmetric distribution through the thickness of the laminate. The external

plies are submitted to a compressive stress distribution and the internal ones to a tensile stress. This time corresponds to the moment when the curvature of the laminate is zero (Fig. 3a). At the time  $t_4$ , the stresses distribution then tends to the steady state stress at RH = 90%, which correspond to time  $t_5$ . An important change in the stresses distribution therefore appears when the material is submitted to important RH after being dried. This change was not monitored by the authors in their previous study [3] as it started from RH = 50% and was submitted to immersion condition.

The evolution of the stresses distribution in the local coordinate system is represented in Fig. 10a and b. As was previously explained, the longitudinal stresses (Fig. 10a) are mostly compressive stresses at the early moments of diffusion (for  $t_0$ ,  $t_1$ ,  $t_2$ ) and turns to tensile stresses when the moisture diffuses and tends to a saturated state (for  $t_4$  and  $t_5$ ). The transversal stresses (Fig. 10b) are mainly tensile stresses at the same early moments and tend to compressive stresses during diffusion due to the swelling of the composite along this direction, which is blocked by the surrounding longitudinal fibers. The impact of moisture content gradients is more visible in this distribution, and notably at times  $t_1$  and  $t_2$  where sharp variations of the stresses distribution are visible near the external plies (around  $z = -0.23$  and  $z = 0.23$  mm). These are due to the important moisture content gradients observed at the same times (Fig. 8b). The symmetry of the stresses distribution is once again found at  $t_3$ , after what the stresses tend to the distribution observed in steady state at RH = 90% (Fig. 7b).

The transversal stress  $\sigma_{22}$  is the more likely to produce defects such as fiber/matrix decohesion, matrix cracking and delamination [26], which were already experimentally observed on flax/PP composites [23,30]. Monitoring its values during moisture diffusion is therefore crucial to ensure optimal performance of the material. The results presented earlier (Fig. 10b) suggest important variations of this stress distribution during sorption. The maximum value of this stress component is plotted in Fig. 11 versus the mean moisture content when submitted to different environmental conditions.

At 0% RH, the maximum stress reaches 26.4 MPa, which was already observed in Figs. 7b and 10b. When imposing incremental RH variations from 0% to 50%, the maximum stress decreases during each interval (0-10%, 10-30% and 30-50%) until it reaches 0 MPa at 50%RH. A further increase in the environmental loading leads to an increase in this maximum value, until it reaches 10 MPa under

steady state immersion. The rise of  $\sigma_{22}$  is however non-monotone. From 50% to 70% RH, it first increases before decreasing and increasing again. From 70% to 90% RH, and from 90% RH to immersion condition, it first decreases before increasing again. These variations are explained by the combined actions of several phenomena:

- the presence of high moisture content gradients, which leads to a heterogeneous behavior of the 90° plies and tends to increase the stresses intensities,
- the decrease in the mechanical properties and the increase of the transversal strain of the plies until a moisture content of 10%,

The evolution of  $\sigma_{22}$  is proposed for two more conditions: when the laminate is initially at 0% or at 50%RH and is submitted to immersion condition. For the first case, the stress is initially at 26.4 MPa and decreases to 19 MPa at  $C = 5\%$ , but then increases until 23MPa at  $C = 10\%$ . It then decreases below 20 MPa at  $C = 12.5\%$  and the curve then follows the results for the segment studied between 90% RH and immersion condition. For the second case, the evolution is similar to the one between 50% and 70%RH, as the stress first rises before decreasing and increasing again by following the curve between 90% RH and immersion conditions. The maximum value reaches 12.4 MPa at  $C = 10\%$ .

It has to be noted that a modification of the diffusion coefficient was investigated to better reproduce the experimental data in Fig. 5a, leading to values of  $D_{zz}$  twice the initial value. However, it showed that the estimated stresses with a modified coefficient only slightly overestimate the initially predicted stresses intensity with less than 5% of modification of the stresses intensity. Therefore, the stresses distributions presented in Figs. 9-11 are considered as representative of the experimentally observed mechanical state.

## 4. Discussion

The moisture sorption of flax/MAPP biocomposite slaved by the hygroscopicity of flax fibers has major consequences on their internal mechanical state. An initially dry MAPP/Flax composite with 60% of fiber volume fraction absorbs in a sigmoidal way around 10% and 31% of moisture when

submitted to RH=90% and water immersion conditions, respectively. Moisture sorption from the dry state (0% RH) to a wet state (90% RH and immersion) implies an exponential decay of the elastic tensile properties (i.e. the in-plane longitudinal, transversal and shear moduli) due to the evolution of flax fiber properties (Fig. 1a, b and c).

Moisture sorption induces anisotropic hygro-expansion (Fig. 2) principally along the transverse direction of flax fibers due to their microstructure (e.g. their microfibril angle). Compared to free fibers, the hygro-expansion of biocomposites is reduced, thus confirming a constraining effect of the matrix on the fiber together with the rise of internal hygroscopic stresses. These hygroscopic stresses are also highlighted by the appearance of a large curvature in an asymmetric lay-up submitted to moisture variations. These hygroscopic stresses lead consequently to a modification of the moisture sorption [3].

The curvature predicted with the presented model in the case of an initially dried asymmetric laminate submitted to various environmental condition is found satisfactory compared to the measured ones, both in transient and in steady-state cases (Fig. 3 a and b, respectively). The predicted curvatures during transient moisture diffusion are in good agreement with the experimentally measured ones, even though they evolve slowly than the measured ones. This might be due to a possible dependence of the moisture diffusion coefficient to the applied environmental condition and the induced hygroscopic stress state, as was already observed in [3].

The application of the developed model to the prediction of the curvature of a similar asymmetric laminate initially at 50% RH and submitted to immersion condition permits to better predict its hygroscopic strain state compared to the initial model [3]. This emphasizes the need to improve the initial model [3] with a more accurate description of the material hygro-mechanical behavior [22], which is the objective of this study. It therefore appears that the properties initially obtained in [3] were not the most capable of describing the hygro-mechanical behavior of the involved material. These properties were indeed identified during transient sorption of the composite submitted to immersion conditions from an initial state under 50% RH. This leads to important moisture content gradients, which might alter the identification of the moisture dependence of the hygro-mechanical properties. The identification of these properties on a composite in a saturated state under various

environmental conditions therefore seems a better way to accurately describe its hygro-mechanical behavior.

**At steady state**, deeper numerical analysis of the involved biocomposite with an asymmetric lay-up evidences that,

- An important tensile stress state is obtained for relative humidity conditions lower than 50% RH (from 0 to 30%), as  $\sigma_{22}$  is comprised between 10 MPa and 26.4 MPa on this environmental condition range. The curvature is relatively low and has an opposite sign compared to the one obtained at higher moisture content.
- For RH conditions higher than 50% RH, the amplitude of the curvature evolves in the opposite way and the tensile stresses remain lower than 10 MPa but they are still above the transverse strength of the flax/MAPP composite.

However, even if higher tensile stresses are observed for the samples submitted to relatively dried condition (i.e. from 0 to 30% RH), which appears as detrimental on the mechanical state, these conditions lead to the highest elastic moduli (Fig. 1). Recent works from Requilé et al. [31] and Gager et al. [32] have shown a non-monotonic evolution of the tensile strength as a function of the relative humidity and moisture content with an optimal tensile strength appearing between 50 and 75% RH conditions on UD epoxy/hemp and non-woven PP/flax composites. Therefore, a detrimental effect of the mechanical state on the material strength may be argued. Indeed, under environmental conditions lower than 50% RH the internal tensile stresses reach high values (i.e. higher than 19 MPa) while above the 50%RH condition, internal stresses rise again and are combined with a moisture induced plasticization effect of cell-walls. A reduction of strength is observed.

**In transient regime**, the internal stresses are numerically evaluated during sorption as a function of time. Different moisture conditions were applied, from 0 to 10% RH, 10 to 30% RH, 30 to 50% RH, 50 to 70% RH, 70 to 90% RH, and 90% RH to immersion. Results evidence complex internal stresses evolution with moisture and time. Indeed, during these environmental loading a combination of actions should appear:

- The presence of high moisture content gradients, which increases the stresses intensities,
- The decrease in the mechanical properties and the increase of the transversal strain of the plies until a moisture content of 10%.

Then, two distinct environmental conditions were numerically applied (i.e. 0 % RH to immersion and 50 % RH to immersion) and their effects on internal stresses  $\sigma_{22}$  were shown. If the immersion condition is directly applied to a sample initially in a dry or ambient condition (i.e. 0% RH or 50% RH, respectively), the stresses intensity might remain important during the first moments of moisture diffusion and highly influenced by the moisture content gradients. Immersion of a previously dried biocomposite should lead to the most detrimental condition of degradation and thus has to be considered when performing aging of natural fiber composite materials or developing hygromorph biocomposites.

## 5. Conclusion

The present study proposes to investigate numerically the development of hygroscopic stresses in a flax fiber reinforced polypropylene matrix composite submitted to different environmental conditions, from the dried state (RH 0%) through various relative humidity conditions (including 10, 30, 50, 70 and 90% RH) to immersion. To this end, a previously developed model has been adapted by taking into account a fine description of the evolution of the hygro-mechanical properties and hygroscopic strains of the composite as a function of the water content. The model is thoroughly validated by comparing the evolution of the estimated curvature of asymmetric laminate with the ones measured experimentally under several environmental conditions. The updated model permits to accurately predict the hygroscopic strains and curvature compared to the initial model.

The stresses distribution through the thickness of the laminate are also estimated under several environmental conditions. It appears that under dry conditions (RH < 30% RH), high transverse tensile stresses  $\sigma_{22}$  are reached (e.g. the maximum value of the transversal stress component  $\sigma_{22}$ , reached 26.4 MPa at 0% RH). These stresses are reduced at 50% RH and then increase again until 90% RH or immersion condition is applied. This non-monotonic evolution of internal stresses may have only a

slight effect on elastic properties but **are** stated to influence drastically the tensile strength of biocomposites. Indeed, the internal stresses overcome the transverse strength of the MAPP/flax unidirectional composite, leading to potential damage. **From the modeling results, it also appears that** a biocomposite stored under 0% RH condition remains submitted to higher internal stresses compared to a 50%RH stored counterpart. A progressive humidification step enables to reduce drastically the stresses intensity with levels lower than 10MPa thanks to lower hygro-mechanical gradients.

## Acknowledgments

The authors wish to warmly thank Dr Johnny Beaugrand from INRA BIA for supplying data of **the** Dynamic Vapor Sorption (DVS) experiments.

## References

- [1] C.A.S. Hill, A. Norton, G. Newman, The Water Vapor Sorption Behavior of Natural Fibers, *J. Appl. Polym. Sci.* 112 (2009).
- [2] A. le Duigou, J. Merotte, A. Bourmaud, P. Davies, K. Belhouli, C. Baley, Hygroscopic expansion: A key point to describe natural fibre/polymer matrix interface bond strength, *Compos. Sci. Technol.* 151 (2017). doi:10.1016/j.compscitech.2017.08.028.
- [3] M. Péron, A. Céline, M. Castro, F. Jacquemin, A. Le Duigou, Study of hygroscopic stresses in asymmetric biocomposite laminates, *Compos. Sci. Technol.* 169 (2019) 7–15. doi:10.1016/j.compscitech.2018.10.027.
- [4] K.M. Almgren, E.K. Gamstedt, Characterization of Interfacial Stress Transfer Ability by Dynamic Mechanical Analysis of Cellulose Fiber Based Composite Materials, *Compos. Interfaces.* 17 (2010) 845–861. doi:10.1163/092764410X539235.
- [5] B.E. Sar, S. Fréour, P. Davies, F. Jacquemin, Coupling moisture diffusion and internal mechanical states in polymers – A thermodynamical approach, *Eur. J. Mech. - A/Solids.* 36 (2012) 38–43. doi:10.1016/j.euromechsol.2012.02.009.
- [6] T. Joffre, E.L.G. Wernersson, A. Miettinen, C.L. Luengo Hendriks, E.K. Gamstedt, Swelling of cellulose fibres in composite materials: Constraint effects of the surrounding matrix, *Compos. Sci. Technol.* 74 (2013) 52–59. doi:10.1016/j.compscitech.2012.10.006.
- [7] A. Céline, S. Fréour, F. Jacquemin, P. Casari, The hygroscopic behavior of plant fibers: a review, *Front. Chem.* 1 (2014) 1–12.
- [8] O. Faruk, A.K. Bledzki, H.-P. Fink, M. Sain, Biocomposites reinforced with natural fibers: 2000–2010, *Prog. Polym. Sci.* 37 (2012) 1552–1596. doi:10.1016/j.progpolymsci.2012.04.003.
- [9] Z.N. Azwa, B.F. Yousif, A.C. Manalo, W. Karunasena, A review on the degradability of polymeric composites based on natural fibres, *Mater. Des.* 47 (2013) 424–442. doi:http://dx.doi.org/10.1016/j.matdes.2012.11.025.
- [10] P.P. Parlevliet, H.E.N. Bersee, A. Beukers, Residual stresses in thermoplastic composites-A

- study of the literature-Part II: Experimental techniques, *Compos. Part A Appl. Sci. Manuf.* 38 (2007) 651–665. doi:10.1016/j.compositesa.2006.07.002.
- [11] M. Gigliotti, J. Molimard, F. Jacquemin, A. Vautrin, On the nonlinear deformations of thin unsymmetric 0/90 composite plates under hygrothermal loads, *Compos. Part A Appl. Sci. Manuf.* 37 (2006) 624–629. doi:10.1016/j.compositesa.2005.05.003.
- [12] O.G. Kravchenko, S.G. Kravchenko, R.B. Pipes, Chemical and thermal shrinkage in thermosetting prepreg, *Compos. Part A Appl. Sci. Manuf.* 80 (2016) 72–81. doi:10.1016/j.compositesa.2015.10.001.
- [13] M.C. Lee, N.A. Peppas, Models of moisture transport and moisture induced stresses in epoxy composites, *J. Compos. Mater.* 27 (1993) 1146–1171.
- [14] A. Benkeddad, M. Grédiac, A. Vautrin, On the transient hygroscopic stresses in laminated composite plates, *Compos. Struct.* 30 (1995) 201–215.
- [15] J. Mercier, A. Bunsell, P. Castaing, J. Renard, Characterization and modeling of aging of composites, *Compos. Part A Appl. Sci. Manuf.* 39 (2008) 428–438.
- [16] P. Vaddadi, T. Nakamura, R.P. Singh, Transient hygrothermal stresses in fiber reinforced composites: a heterogeneous characterization approach, *Compos. Part A Appl. Sci. Manuf.* 34 (2003) 719–730.
- [17] G. Youssef, S. Fréour, F. Jacquemin, Stress-dependent moisture diffusion in composite materials, *J. Compos. Mater.* 43 (2009) 1621–1637.
- [18] D. Jain, A. Mukherjee, N. Kwatra, Effect of fibre topology on hygro-mechanical response of polymer matrix composites, *Int. J. Heat Mass Transf.* 86 (2015) 787–795.
- [19] H. Obeid, A. Clément, S. Fréour, F. Jacquemin, P. Casari, On the identification of the coefficient of moisture expansion of polyamide-6: Accounting for differential swelling strains and plasticization, *Mech. Mater.* 118 (2018) 1–10.
- [20] A. Regazzi, R. Léger, S. Corn, P. Jenny, Modeling of hydrothermal aging of short flax fiber reinforced composites, *Compos. Part A Appl. Sci. Manuf.* 90 (2016) 559–566.
- [21] A. Chilali, M. Assarar, W. Zouari, H. Kebir, R. Ayad, Analysis of the hydro-mechanical behaviour of flax fibre-reinforced composites: Assessment of hygroscopic expansion and its impact on internal stress, *Compos. Struct.* 206 (2018) 177–184. doi:10.1016/j.compstruct.2018.08.037.
- [22] A. Le Duigou, V. Keryvin, J. Beaugrand, M. Pernes, F. Scarpa, Humidity responsive actuation of bioinspired hygromorph biocomposites ( HBC ) for adaptive structures, *Compos. Part A.* 116 (2019) 36–45. doi:10.1016/j.compositesa.2018.10.018.
- [23] M. Le Duigou, A., Castro, Hygromorph BioComposites : Effect of fibre content and interfacial strength on the actuation performances, *Ind. Crop Prod.* 99 (2017) 142–149.
- [24] A Le Duigou, S Requile, J Beaugrand, F Scarpa, M Castro, Natural fibres actuators for smart bio-inspired hygromorph biocomposites, *Smart Mater. Struct.* 26 (2017).
- [25] Z. El Hachem, A. Céline, G. Challita, M.-J. Moya, S. Fréour, Hygroscopic multi-scale behavior of polypropylene matrix reinforced with flax fibers, *Ind. Crops Prod.* 140 (2019).
- [26] C.T. Herakovich, *Mechanics of fibrous composites*, John Wiley & Sons, 1998.
- [27] M.W. Hyer, Calculations of the Room-Temperature Shapes of Unsymmetric Laminates, *J. Compos. Mater.* 15 (1981) 296.
- [28] M. Berges, R. Léger, V. Placet, V. Person, S. Corn, X. Gabrion, J. Rousseau, E. Ramasso, P.

- Ienny, S. Fontaine, Influence of moisture uptake on the static, cyclic and dynamic behaviour of unidirectional flax fibre-reinforced epoxy laminates, *Compos. Part A Appl. Sci. Manuf.* 88 (2016) 165–177.
- [29] E.H. Saidane, D. Scida, M. Assarar, R. Ayad, Effects of manufacturing process and water ageing on the mechanical behaviour of two reinforced composites: Flax-fibres and glass-fibres, in: *Proc. 16th Eur. Conf. Compos. Mater. ECCM*, 2014.
- [30] A. Le Duigou, A. Bourmaud, C. Baley, In-situ evaluation of flax fibre degradation during water ageing, *Ind. Crops Prod.* 70 (2015) 204–210. doi:10.1016/j.indcrop.2015.03.049.
- [31] S. Réquillé, A. Le Duigou, A. Bourmaud, C. Baley, Deeper insights into the moisture induced hygroscopic and mechanical properties of hemp reinforced biocomposites, *Compos. Part A Appl. Sci. Manuf.* 123 (2019) 278–285.
- [32] V. Gager, A. Le Duigou, A. Bourmaud, P. Floran, K. Behlouli, C. Baley, Understanding the effect of moisture variation on the hygromechanical properties of porosity-controlled nonwoven biocomposites, *Polym. Test.* 78 (2019).

## Figures caption

Figure 1: Evolution of the measured and approximated mechanical properties of the composite a)  $E_L$  b)  $E_T$  c)  $G_{LT}$ , adapted from [22].

Figure 2: Evolution of the measured in-plane hygroscopic strains  $\varepsilon^{hyg}$  from [3][22].

Figure 3: Measured and modelled curvature of the composite for the different environmental conditions a) evolution with time b) maximum value versus moisture content at saturation.

Figure 4: Evolution of the curvature obtained on an asymmetric laminate initially under 50%RH submitted to immersion condition. Comparison of the results obtained experimentally [3], with the initial model [3] and with the adapted model.

Figure 5: Stresses distribution through the thickness of the laminate in the global coordinate system for several environmental conditions a) Main component along the x direction b) Main component along the y direction.

Figure 6: Global and local coordinate systems.

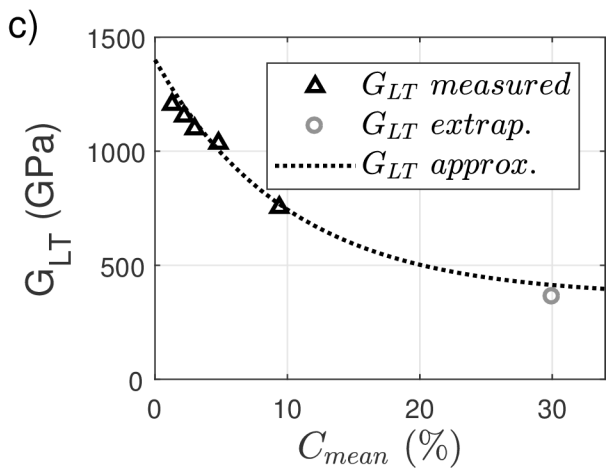
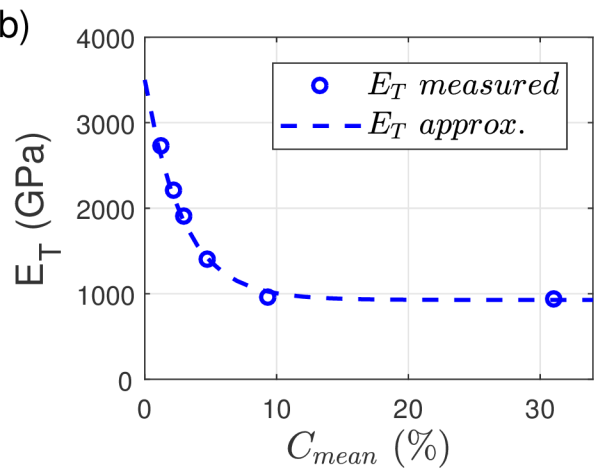
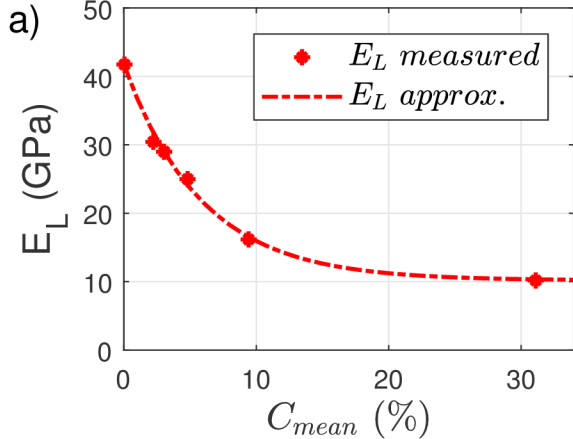
Figure 7: Stresses distribution through the thickness of the laminate in the local coordinate system for several environmental conditions a) Main component along the fiber direction 1 b) Main component along the transversal direction 2.

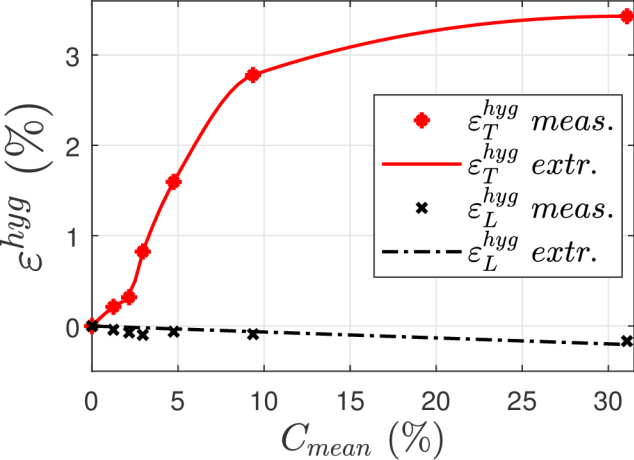
Figure 8: Estimated moisture uptake from dry state to saturation under 90% RH a) Mean moisture content  $C_{mean}$  during saturation b) Moisture distribution through the laminate thickness for several times  $t_i$ .

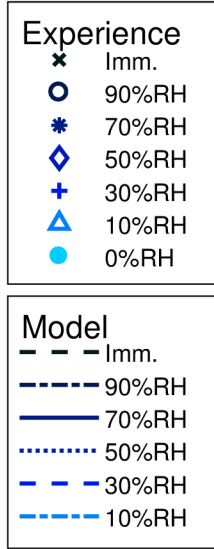
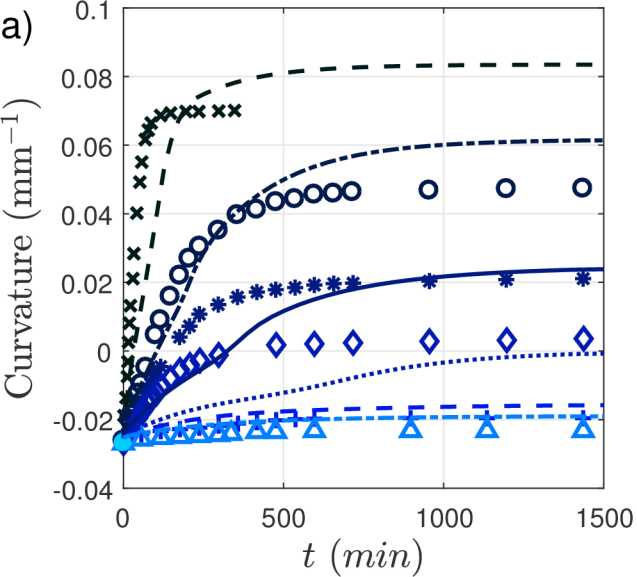
Figure 9: Stresses distribution through the thickness of the laminate in the global coordinate system for each  $t_i$  during the moisture diffusion from RH 0% to RH 90% a) Main component along the x direction b) Main component along the y direction.

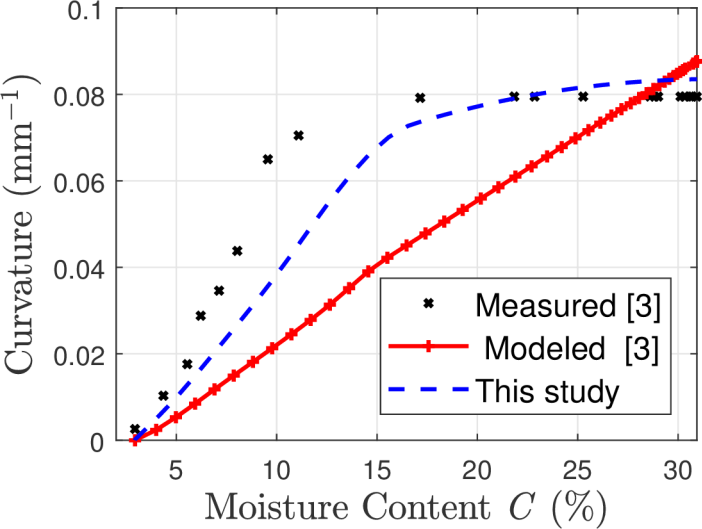
Figure 10: Stresses distribution through the thickness of the laminate in the local coordinate system for different times  $t_i$  during the moisture diffusion from RH 0% to RH 90% a) Main component along the fiber direction 1 b) Main component along the transversal direction 2.

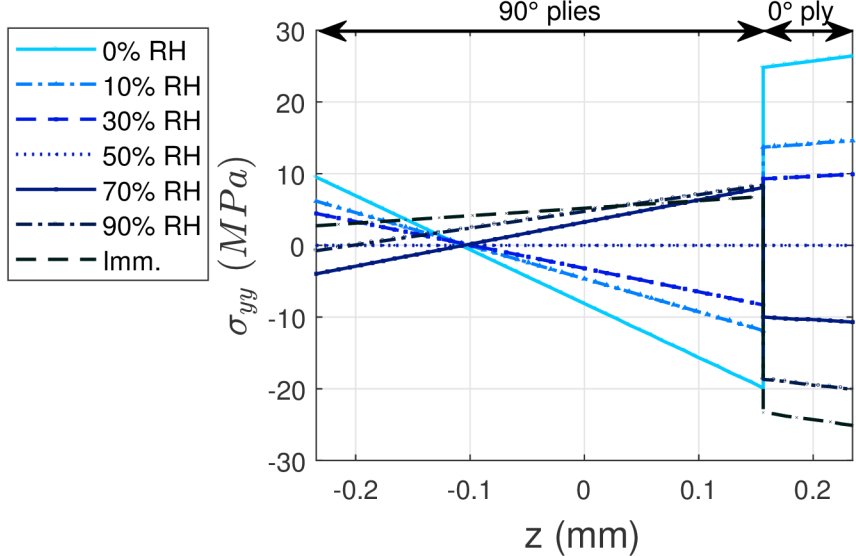
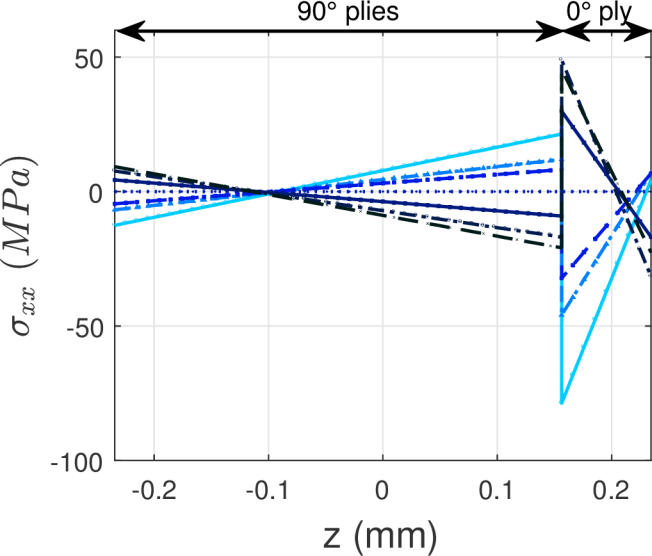
Figure 11: Evolution of the maximal transverse stress  $\sigma_{22}$  with moisture content  $C$  for several environmental conditions.

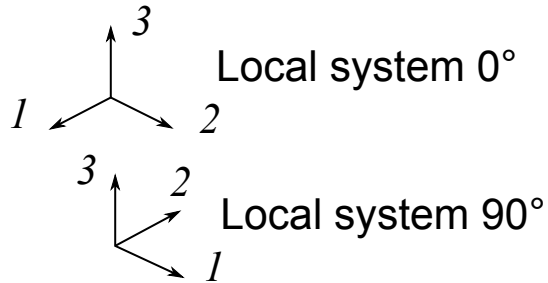
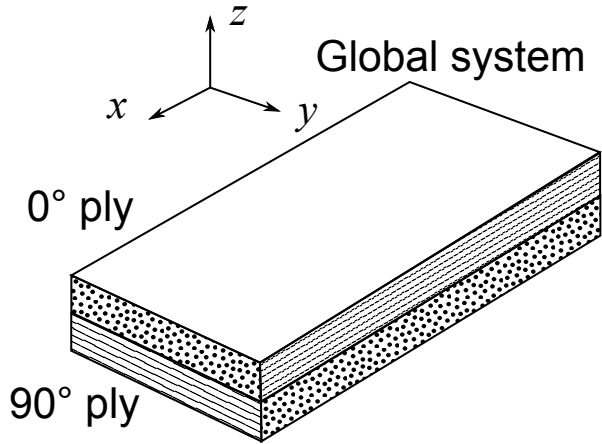


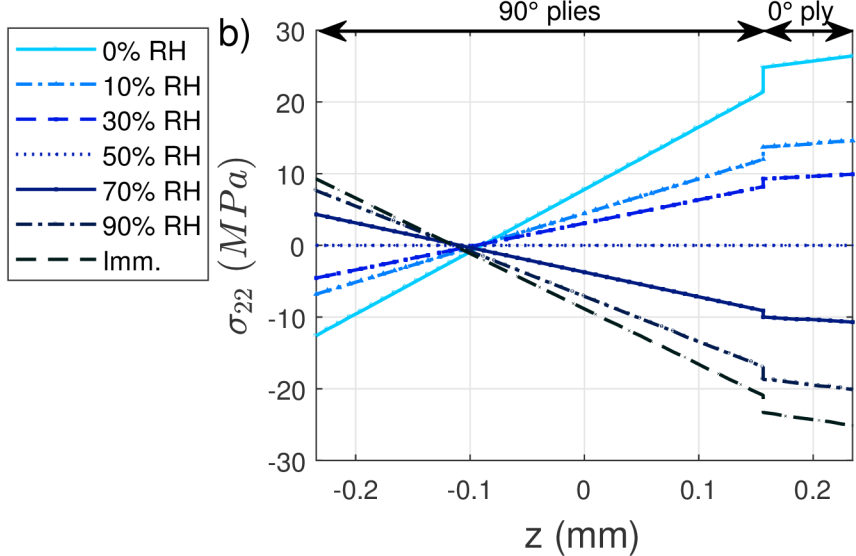
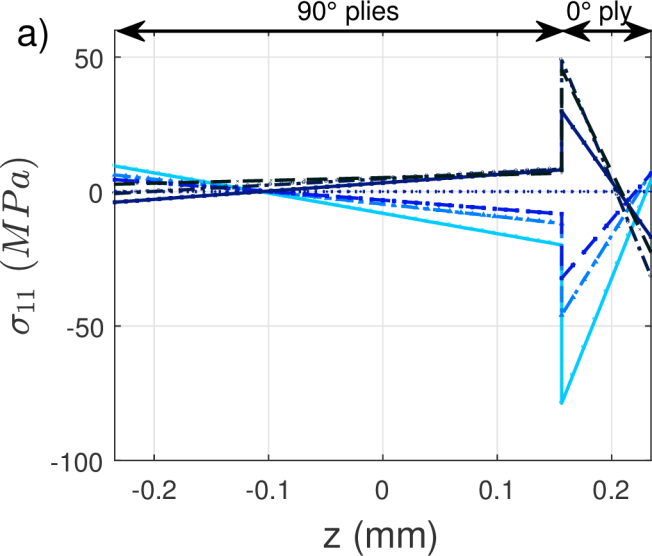


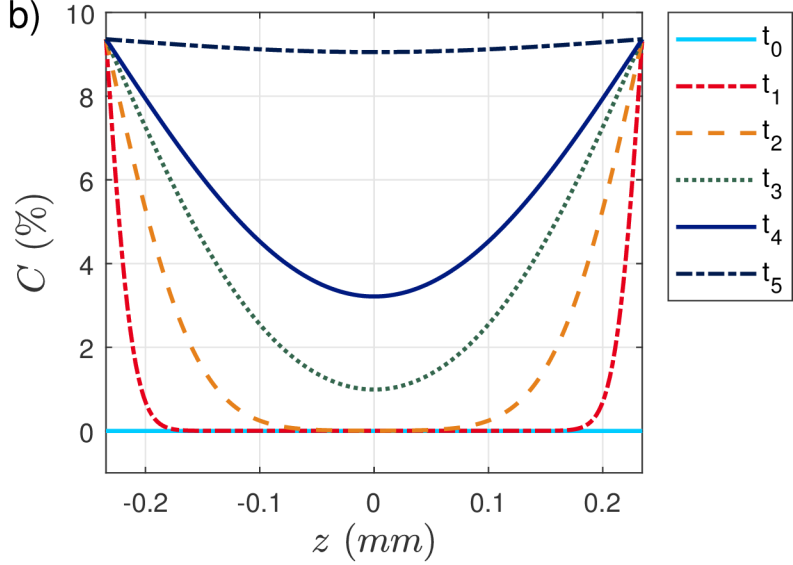
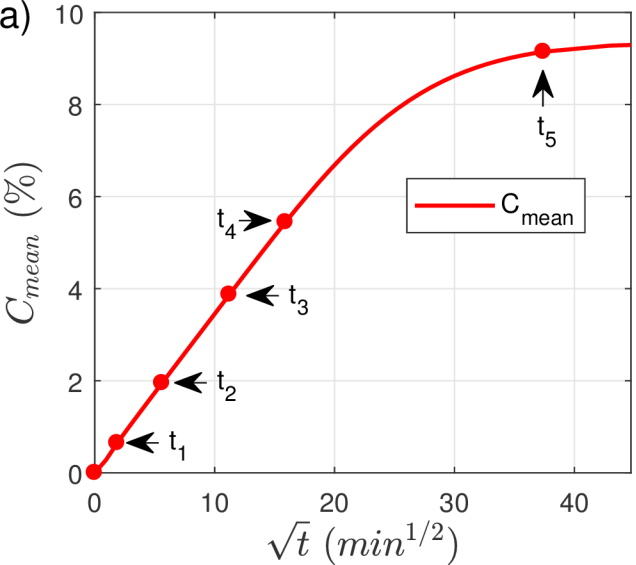


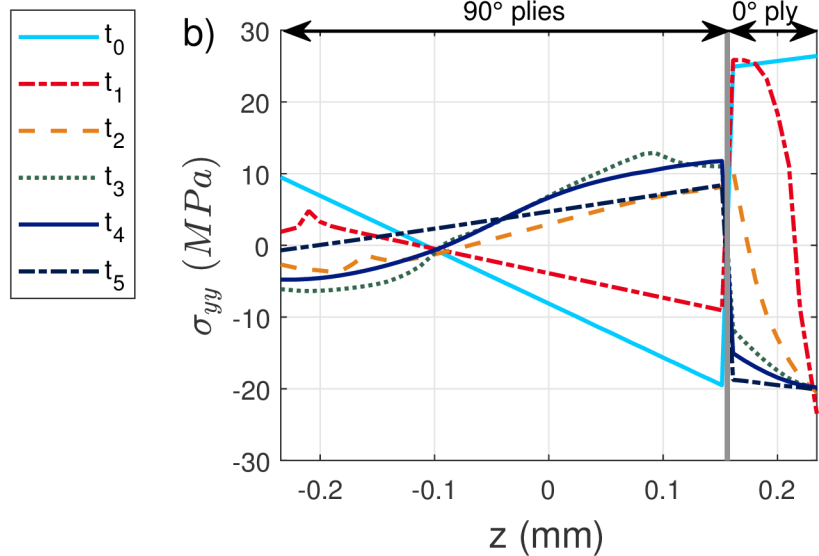
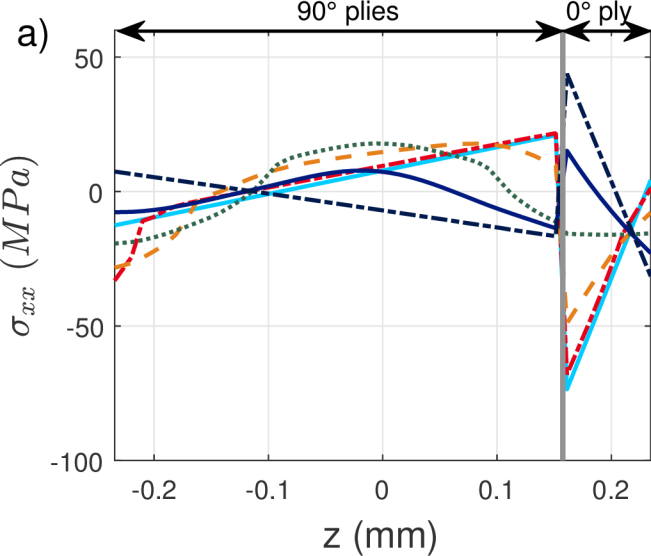


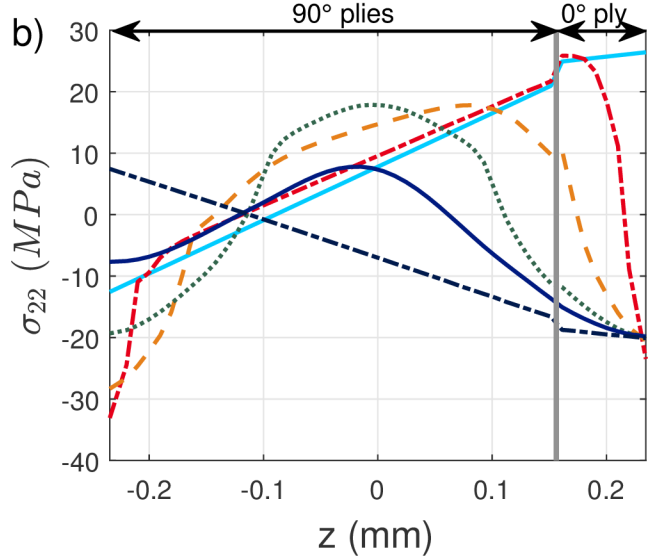
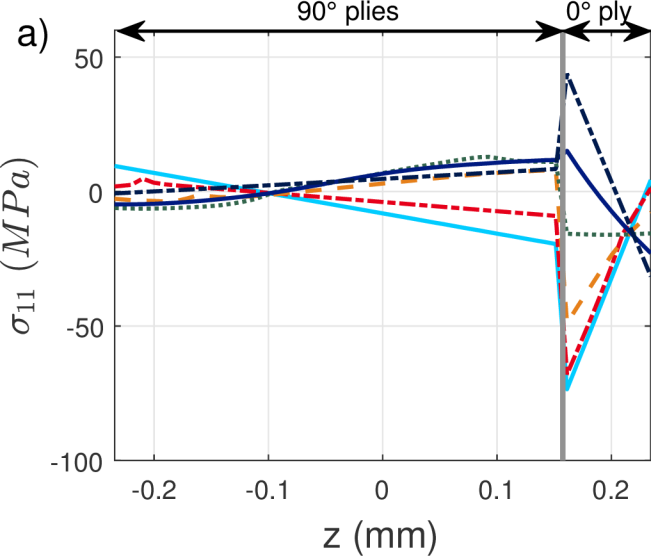














## Tables

Table 1: Stabilized moisture content obtained under several environmental conditions

<i>Condition</i>	<i>0% RH</i>	<i>10% RH</i>	<i>30% RH</i>	<i>50% RH</i>	<i>70% RH</i>	<i>90% RH</i>	<i>Immersion</i>
$M_{RH}$ (%)	0	1.24	2.15	2.95	4.75	9.36	31.1

Table 2: Parameters of the fitting functions for  $E_L$ ,  $E_T$  and  $G_{LT}$ .

Property	Unit	Value
$E_{Lmax}$	(MPa)	41490
$E_{Lmin}$	(MPa)	10180
$E_{Tmax}$	(MPa)	3500
$E_{Tmin}$	(MPa)	928
$G_{LTmax}$	(MPa)	1400
$G_{LTmin}$	(MPa)	362

Table 3: Specific times  $t_i$ .

$t_i$	$t_0$	$t_1$	$t_2$	$t_3$	$t_4$	$t_5$
Value (min)	0	3.5	31.5	126	253	1400